Nonlinear Analysis: Modelling and Control, Vol. 28, No. 2, 194–208
https://doi.org/10.15388/namc.2023.28.30563

Existence theories and exact solutions of nonlinear PDEs dominated by singularities and time noise

Muhammad Ozair Ahmed[a], **Rishi Naeem**[b], **Muhammad Akhtar Tarar**[c], **Muhammad Sajid Iqbal**[b], **Mustafa Inc**[d,e,1], **Farkhanda Afzal**[b]

[a]Department of Mathematics, Statistics,
The University of Lahore,
54000, Lahore, Pakistan
drchadury@yahoo.com

[b]Department of Humanities & Basic Sciences,
Military College of Signals, NUST,
Islamabad, Pakistan
rishinaeem@mcs.edu.pk; sajid606@gmail.com;
m_sajid_iqbal@mcs.edu.pk; farkhanda@mcs.edu.pk

[c]Civil Engineering, The University of Lahore,
54000, Lahore, Pakistan
akhtartarar2000@yahoo.com

[d]Department of Mathematics, Science Faculty,
Firat University,
23119, Elazig, Turkey
minc@firat.edu.tr

[e]Department of Medical Research,
China Medical University,
40402 Taichung, Taiwan

Received: August 7, 2022 / **Revised:** December 22, 2022 / **Published online:** January 9, 2023

Abstract. The current research deals with the exact solutions of the nonlinear partial differential equations having two important difficulties, that is, the coefficient singularities and the stochastic function (white noise). There are four major contributions to contemporary research. One is the mathematical analysis where the explicit a priori estimates for the existence of solutions are constructed by Schauder's fixed point theorem. Secondly, the control of the solution behavior subject to the singular parameter ϵ when $\epsilon \to 0$. Thirdly, the impact of noise that is present in the differential equation has been successfully handled in exact solutions. The final contribution is to simulate the exact solutions and explain the plots.

Keywords: singular partial differential equations, noise function, exact solutions, Schauder's fixed point theorem, a priori estimates.

[1]Corresponding author.

1 Introduction

There are mainly two types of partial differential equations, one can be said as the classical, and the other is known as the stochastic partial differential equation. The fundamental difference is that the classical partial differential equation always possesses the smooth solutions, and hence they govern the physical environment where the solutions statics must be regular enough. Such problems are important but less applicable. On the other hand, the stochastic partial differential equations carrying the noise (white) have mathematical difficulties but they are the representation of actual physical states. As a result, the consideration of physical problems governed by the stochastic partial differential equations demands high level of mathematical understanding and their handling in comparatively different environment such as Sobolev spaces instead of classical topological spaces. These differential equations are one of the main research areas and play a very significant role in practical applications, provided that we use it as an appropriate mathematical model [2, 26, 27, 29]. Most of complex systems, natural or artificial, can be modeled using these equations. Generally, the nonlinear partial differential equations are the classical ones and cannot easily be solved. On the other hand, the solutions of nonclassical partial differential equations i.e., stochastic partial differential equations, may have complexities when they break smoothness, and in this case, it is not easy to find the bound of the solutions as compare to classical ones. So we need different analytical techniques to find the solutions. There are many available techniques to find the solutions (see [1, 4–8, 10–13, 15–25, 28, 30, 32, 34, 35]), and we use Ricatti–Bernoulli sub-ODE method [31], and the details can be seen in the coming sections. This article is based on a second-order partial differential equation [14], where the desired solutions u depend on x and t. The coefficients of u are $1/\epsilon^2$ and $\dot{W}$. $1/\epsilon^2$ represents the singular linearity perturbation of the superconductivity in the multiscale circumstances. The coefficient $\dot{W}$ is the noise function, and it is generated by a Q-Wiener process with small noise intensity. The presence of the parameter ϵ and the multiplicative noise $\dot{W}$ result in a state, which is comparatively difficult for analysis. The main aim of this article is to find the solutions to the said partial differential equation and simulation of obtained results. In the next section, statement of the problem is given, and the existence of the solutions is examined. Section 3 deals with the methodology and stochasticity. The mathematical formulas of the solution of required problem are given in Section 4. The surface and contour plots of obtained results are given in Section 5.

2 Statement of problem

The main goal of the complete article is to solve the following stochastic partial differential equation exactly:

$$\frac{\partial u}{\partial t} = \frac{1}{\epsilon^2}\frac{\partial^2 u}{\partial x^2} + \frac{1}{\epsilon^2}u + \kappa u^2 + \epsilon u\dot{W}. \tag{1}$$

There are two complexities to the problem. One is the singularity of the coefficient, and the second complexity is the presence of multiplicative noise. Since the multiplicative noise is present in the said problem, the smoothness has been compromised of the solutions of partial differential equation. The idea is to find the solutions profile in the form of simulation so that the spikes/nonsmoothness should be controlled, and the solutions must describe the physical phenomena. For this purpose, we use the Ricatti–Bernoulli sub-ODE method, and then we simulate our results.

2.1 Existence results

We consider the partial differential equation (1) with the initial condition

$$u(x,0) = u_0 x. \tag{2}$$

The solution $u(x,t)$ of PDE (1) can be written by using the first integration with respect to t as follows:

$$u = u_0(x) + \int_0^t \left(\frac{1}{\epsilon^2}u_{xx} + \frac{1}{\epsilon^2}u + \kappa u^2 + \epsilon u\dot{W}\right)(x,\tau)\,\mathrm{d}\tau. \tag{3}$$

Then the following operator

$$U = u_0(x) + \int_0^t \left(\frac{1}{\epsilon^2}u_{xx} + \frac{1}{\epsilon^2}u + \kappa u^2 + \epsilon u\dot{W}\right)(x,\tau)\,\mathrm{d}\tau \tag{4}$$

is the fixed point operator reduction of (1) and (2).

The fundamental goal of the current studies is to show the existence of the solution of the underlying problem with the presence of noise in the physical problem by applying Schauder's fixed point theorem [3, 9] stated as follows.

Theorem 1 [Schauder's fixed point theorem]. *Suppose that $U : B \to B$ is a continuous self-map, where B is a closed, convex and bounded subset of a Banach space. If the image of U under B is precompact, then U has at least one fixed point in B.*

Naturally, we cannot work in the classical environment of analysis. Here we consider the Lebesgue space as the Banach space. So we shall consider the Banach space $L_2[0,\rho]$ equipped with L_2 norm. Also, we construct the following closed, convex and bounded subset in the function space $L_2[0,\rho]$:

$$B_r(\Theta) = \bigl\{u, u \in L_2[0,\rho]\colon \|u\|_{L_2[0,\rho]} \leqslant r\bigr\}, \tag{5}$$

where Θ is the zero element of the function space, that is, $\|\Theta - u\| = \|u - \Theta\| = \|u\|$, and r is the radius of open ball to be optimized.

We shall apply the Schauder fixed point theorem to show the existence in the $L_2[0,\rho]$ space. Consequently, we have to test two conditions:

(i) Self-mapping, that is, U in (4) maps (5) into itself $U : B_r(\Theta) \to B_r(\Theta)$.
(ii) $U(B_r(\Theta))$ is relatively compact.

For first condition, we take the L_2 norm of equation (4), and we get

$$\|U\| \leqslant \big\|u_0(x)\big\| + \left\| \int_0^t \left(\frac{1}{\epsilon^2} u_{xx} + \frac{1}{\epsilon^2} u + \kappa u^2 + \epsilon u \dot{W} \right)(x,\tau)\,\mathrm{d}\tau \right\|.$$

The initial conditions are always bounded, so $\|u_0(x)\| \leqslant \alpha$,

$$\begin{aligned} \|U\| &\leqslant \alpha + \left\| \int_0^t \left(\frac{1}{\epsilon^2} u_{xx} + \frac{1}{\epsilon^2} u + \kappa u^2 \right)(x,\tau)\,\mathrm{d}\tau \right\| + \left\| \epsilon \int_0^t u \frac{\mathrm{d}W}{\mathrm{d}\tau}\,\mathrm{d}\tau \right\|, \\ &= \alpha + \|I_1\| + \|I_2\|. \end{aligned}$$

I_1 can be estimated by integrating continuous functions and using the triangle inequality:

$$\|I_1\| \leqslant \int_0^t \left(\frac{1}{\epsilon^2} \|u_{xx}\| + \frac{1}{\epsilon^2} \|u\| + \kappa \|u\|^2 \right) \mathrm{d}\tau,$$

where $\|u_{xx}\| \leqslant \beta$, $\|u\| \leqslant r$ and $\|u^2\| = \|u\|^2 \leqslant r^2$,

$$\|I_1\| \leqslant \int_0^t \frac{1}{\epsilon^2} \big(\beta + r + \epsilon\kappa r^2\big)\,\mathrm{d}\tau = \frac{\rho}{\epsilon^2} \big(\beta + r + \epsilon\kappa r^2\big),$$

where $\rho = t - 0$;

$$\|I_2\| = \epsilon \left\| \int_0^t u \frac{\mathrm{d}W}{\mathrm{d}\tau}\,\mathrm{d}\tau \right\| \leqslant \epsilon \left\| \int_0^t u\,\mathrm{d}W \right\| \leqslant \epsilon r \int_0^t \mathrm{d}W.$$

Since W is a random function of time, so the integral $\int_0^t \mathrm{d}W$ remains bounded but not equal to ρ necessarily. But since the integral is bounded up to measurable scale, so it can be treated as skewed estimation of ρ, that is, $\int_0^t \mathrm{d}W = \gamma\rho$. So, finally,

$$\|U\| \leqslant \alpha + \frac{\rho}{\epsilon^2} \big(\beta + r + \epsilon\kappa r^2\big) + \epsilon\rho r\gamma = \alpha + \frac{1}{\epsilon^2} \big(\beta + r + \epsilon\kappa r^2 + \epsilon^3 r\gamma\big)\rho.$$

For self-mapping $r > \alpha$,

$$\rho \leqslant \frac{\epsilon^2 (r - \alpha)}{\beta + \epsilon\kappa r^2 + (\epsilon^3\gamma + 1) r}. \tag{6}$$

For weak compactness, we consider the family of images U_i corresponding to the preimages u_i, $i = 1, 2, \dots$, in the fixed point operator equation (4),

$$U_i = u_0(x) + \int_0^t \left(\frac{1}{\epsilon^2} u_{ixx} + \frac{1}{\epsilon^2} u_i + \kappa u_i^2 + \epsilon u_i \dot{W} \right)(x,\tau)\,\mathrm{d}\tau.$$

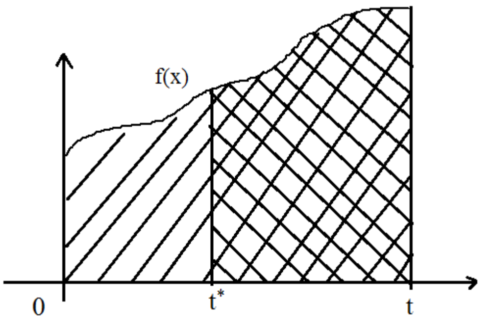

Figure 1. Difference of integrals.

For relatively compactness, the following difference is to be considered:

$$U_i(x,t) - U_i(x,t^*) = \int_0^t \left(\frac{1}{\epsilon^2}u_{ixx} + \frac{1}{\epsilon^2}u_i + \kappa u_i^2 + \epsilon u_i \dot{W}\right)(x,\tau)\,\mathrm{d}\tau$$
$$- \int_0^{t^*} \left(\frac{1}{\epsilon^2}u_{ixx} + \frac{1}{\epsilon^2}u_i + \kappa u_i^2 + \epsilon u_i \dot{W}\right)(x,\tau)\,\mathrm{d}\tau,$$

$$U_i(t) - U_i(t^*) = \int_{t^*}^t \left(\frac{1}{\epsilon^2}u_{ixx} + \frac{1}{\epsilon^2}u_i + \kappa u_i^2 + \epsilon u_i \dot{W}\right)(x,\tau)\,\mathrm{d}\tau,$$

$$\left\|U_i(t) - U_i(t^*)\right\| \leqslant \int_{t^*}^t \left\|\frac{1}{\epsilon^2}u_{ixx} + \frac{1}{\epsilon^2}u_i + \kappa u_i^2 + \epsilon u_i \dot{W}\right\|\mathrm{d}\tau,$$
$$\leqslant \frac{1}{\epsilon^2}\left(\beta + r + \epsilon^2\kappa r^2\right)|t - t^*|.$$

Clearly, $U_i(t) \to U_i(t^*)$ as $t \to t^*$ irrespective of the domain of convergence. So $U_i(t)$, as family of functions, converges to $U_i(t^*)$. That is, $U_i(t)$ is equicontinuous.

So by Arzelà–Ascoli theorem, this equicontinuous family U_i must possesses a subsequence U_{i_j}, which is uniformly convergent, and if we are able to search such a subsequence, then the operator U is relatively compact or, more precisely, $U(B_r(\Theta))$ is relatively compact. Hence by the Schauder's fixed point theorem, there must exists at least one (solution) fixed point of U, which turns out to be the solution of the given problem. To sum up, we have proved the following theorem.

Theorem 2. *Suppose u and all its derivatives are L_2 functions in time variable, then the nonlinear problem* (3) *for stochastic partial differential equations is solvable for Schauder fixed point theorem, and the solvability condition is given by inequality* (6) *subject to additional constraint $r > \alpha$.*

Corollary 1. *The corresponding optimal value for the radius of the ball is*

$$1 + \sqrt{\alpha^2 + \frac{1}{\epsilon^2 \kappa}\bigl(\beta + \alpha(\epsilon\gamma + 1)\bigr)}.$$

Remark 1 [Singularity control]. To verify the control with respect to the singularity ϵ, we have checked that the limit $\epsilon \to 0$ leads $\epsilon^2(r-\alpha)/(\beta + \epsilon\kappa r^2 + (\epsilon^3\gamma + 1)r) \to 0$. Hence the small value of ϵ are acceptable for the continuity of the solution.

3 Methodology

Suppose a nonlinear partial differential equation is written as

$$p(u, u_t, u_x, u_{xx}, u_{xt}, \dots) = 0, \tag{7}$$

where p is in general a polynomial function of its arguments, the subscripts represent the partial derivatives. There are three steps of the Ricatti–Bernoulli sub-ODE method.

Step 1. The variable ξ has been assigned to x and t, i.e.,

$$\xi = kx + \nu t \tag{8}$$

with

$$u(x,t) = U(\xi). \tag{9}$$

With the help of equations (8) and (9), equation (7) is written as

$$p\bigl(U, U', U'', U''', \dots\bigr) = 0, \tag{10}$$

where $U' = \partial U/\partial \xi$.

Step 2. Now assume that the solutions of equation (10) is the solutions of Ricatti–Bernoulli equation

$$U' = aU^{2-m} + bU + cU^m, \tag{11}$$

where a, b, c and m are constants. Equation (11) implies

$$\begin{aligned}
U'' &= ab(3-m)U^{2-m} + a^2(2-m)U^{3-2m} + mc^2U^{2m-1} \\
&\quad + bc(m+1)U^m + (2ac + b^2)U, \\
U''' &= (ab(3-m)(2-m)U1 - m + a^2(2-m)(3-2m)U^{2-2m} \\
&\quad + m(2m-1)c^2U^{2m-2} + bcm(m+1)U^{m-1} + (2ac + b^2))U', \\
&\dots .
\end{aligned}$$

For further details, please see [31].

Equation (11) has the following solutions.

Case 1. When $m = 1$, the solution of equation (11) is

$$U(\xi) = C\mathrm{e}^{(a+b+c)\xi}.$$

Case 2. When $m \neq 1$, $b = 0$ and $c = 0$, the solution of equation (11) is

$$U(\xi) = \bigl(a(m-1)(\xi + C)\bigr)^{1/(m-1)}. \tag{12}$$

Case 3. If $m \neq 1$, $b \neq 0$ and $c = 0$, then the solution of equation (11) is

$$U(\xi) = \left(-\frac{a}{b} + C\mathrm{e}^{b(m-1)\xi}\right)^{1/(m-1)}.$$

Case 4. If $m \neq 1$, $a \neq 0$ and $b^2 - 4ac < 0$, then the solutions of equation (11) are

$$U(\xi) = \left(-\frac{b}{2a} + \frac{\sqrt{4ac - b^2}}{2a} \tan\left(\frac{(1-m)\sqrt{4ac - b^2}}{2}\right)(\xi + C)\right)^{1/(1-m)}$$

and

$$U(\xi) = \left(-\frac{b}{2a} - \frac{\sqrt{4ac - b^2}}{2a} \cot\left(\frac{(1-m)\sqrt{4ac - b^2}}{2}\right)(\xi + C)\right)^{1/(1-m)}.$$

Case 5. If $m \neq 1$, $a \neq 0$ and $b^2 - 4ac > 0$, then the solutions of equation (11) are

$$U(\xi) = \left(-\frac{b}{2a} - \frac{\sqrt{b^2 - 4ac}}{2a} \coth\left(\frac{(1-m)\sqrt{b^2 - 4ac}}{2}\right)(\xi + C)\right)^{1/(1-m)}$$

and

$$U(\xi) = \left(-\frac{b}{2a} - \frac{\sqrt{b^2 - 4ac}}{2a} \tanh\left(\frac{(1-m)\sqrt{b^2 - 4ac}}{2}\right)(\xi + C)\right)^{1/(1-m)}.$$

Case 6. If $m \neq 1$, $a \neq 0$ and $b^2 - 4ac = 0$, then the solution of equation (11) is

$$U(\xi) = \left(\frac{1}{a(m-1)(\xi + C)} - \frac{b}{2a}\right)^{1/(1-m)}.$$

4 Application of method and mathematical formulation of solutions

Suppose that Riccati–Bernoulli equation is the solution of equation (1). Now applying the transformation $u(x,t) = U(\xi)$ with $\xi = kx + \nu t$, (1) becomes

$$\begin{aligned}
&\bigl[\epsilon^2 a\nu - k^2 ab(3-m)\bigr]U^{2-m} - k^2 a^2 (2-m) U^{3-2m} \\
&\quad - k^2 c^2 m U^{2m-1} + \bigl[\epsilon^2 c\nu - k^2 bc(m+1)\bigr]U^m \\
&\quad - \kappa\epsilon^2 U^2 + \bigl[\epsilon^2 b\nu - k^2\bigl(2ac + b^2\bigr) - \epsilon^3 \dot{W} - 1\bigr]U = 0.
\end{aligned}$$

We get the following solutions of (1).

Case 1. If $m = 1$, then

$$u(x,t) = C\mathrm{e}^{(kx+\nu t)(\nu\epsilon^2 \pm k\sqrt{(k+2)(k-2)-4\epsilon^3\dot{W}})/2k^2}.$$

Case 2. If $m = 0$, $c = b = 0$, then

$$u(x,t) = \frac{-\nu}{\kappa(kx+\nu t+C)}.$$

Case 3. If $m \neq 1$, $b \neq 0$ and $c = 0$, we chose $m = 0$, and hence we get $a = 0$, $\kappa = 0$ and $b = (\epsilon^2\nu \pm \sqrt{(\epsilon^2\nu - 2k)(\epsilon^2\nu + 2k) - 4k^2\epsilon^3\dot{W}})/2k^2$. The solutions in this case are

$$u(x,t) = \left(C\mathrm{e}^{-(kx+\nu t)(\epsilon^2\nu \pm \sqrt{(\epsilon^2\nu-2k)(\epsilon^2\nu+2k)-4k^2\epsilon^3\dot{W}})/2k^2}\right)^{-1}.$$

Case 4. If $m \neq 1$, $a \neq 0$ and $\nu^2\epsilon^4 + 2k^2(1+\epsilon^3\dot{W}) < 0$ and $A = \sqrt{-\nu^2\epsilon^4 - 2k^2(1+\epsilon^3\dot{W})}$, then

$$u(x,t) = \left(\frac{-\epsilon^2\kappa}{2(1+\epsilon^3\dot{W})} + \frac{\kappa A}{2\nu(1+\epsilon^3\dot{W})}\tan\left(-\frac{1}{2k^2}A(kx+\nu t+C)\right)\right)^{-1}$$

and

$$u(x,t) = \left(\frac{-\epsilon^2\kappa}{2(1+\epsilon^3\dot{W})} + \frac{\kappa A}{2\nu(1+\epsilon^3\dot{W})}\cot\left(-\frac{1}{2k^2}A(kx+\nu t+C)\right)\right)^{-1}.$$

Case 5. If $m \neq 1$, $a \neq 0$ and $\nu^2\epsilon^4 + 2k^2(1+\epsilon^3\dot{W}) > 0$ and $B = \sqrt{\nu^2\epsilon^4 + 2k^2(1+\epsilon^3\dot{W})}$, then

$$u(x,t) = \left(\frac{-\epsilon^2\kappa}{2(1+\epsilon^3\dot{W})} + \frac{\kappa B}{2\nu(1+\epsilon^3\dot{W})}\coth\left(-\frac{1}{2k^2}B(kx+\nu t+C)\right)\right)^{-1}$$

and

$$u(x,t) = \left(\frac{-\epsilon^2\kappa}{2(1+\epsilon^3\dot{W})} + \frac{\kappa B}{2\nu(1+\epsilon^3\dot{W})}\tanh\left(-\frac{1}{2k^2}B(kx+\nu t+C)\right)\right)^{-1}.$$

Case 6. If $m \neq 1$, $a \neq 0$ and $\nu^2\epsilon^4 + 2k^2(1+\epsilon^3\dot{W}) = 0$, then

$$u(x,t) = \left(\frac{k^2\kappa}{\nu(1+\epsilon^3\dot{W})(kx+\nu t+C)} - \frac{\epsilon^2\kappa}{2(1+\epsilon^3\dot{W})}\right)^{-1}.$$

5 Simulations

This section consists of simulations of the obtained solutions. Figures 2–7 are the surface and contour plots of the solutions $u(x,t)$, which have been obtained in the previous section.

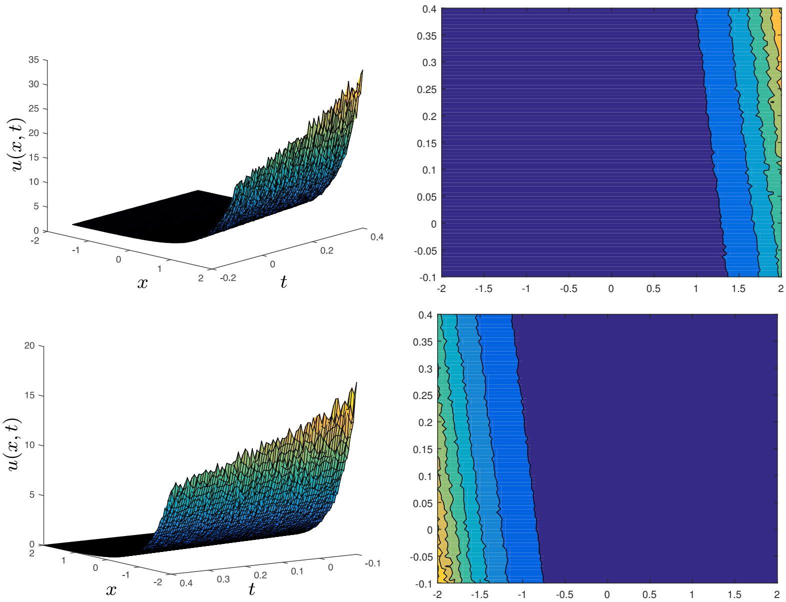

Figure 2. The surface and contour plots of $u(x,t)$ for Case 1.

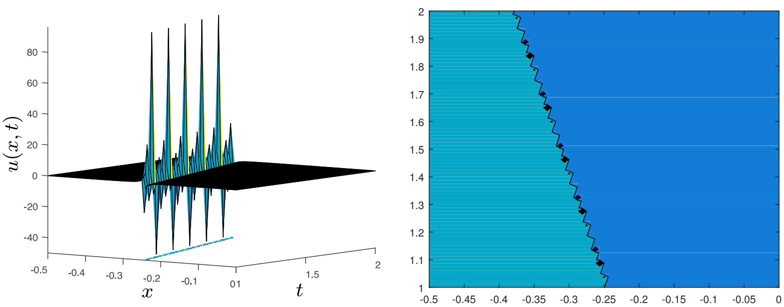

Figure 3. The surface and contour plots of $u(x,t)$ for Case 2.

- Figure 2: Case 1 of $u(x,t)$ consists of parameters k, ν, ϵ and C. We chose $\nu = 3$, $C = .5$, $k = 4$, $\epsilon = .4$, and the resulting exponential graphs and contour plots for Case 1 are shown in this figure.
- Figure 3: The second case consists of the parameter k, κ, ν and C. The values that we chose for these parameters are $\nu = 1.2$, $C = 1$, $k = 9$, $\kappa = 10$, and the corresponding plots are shown there.
- Figure 4: The third, fourth, fifth and sixth case consist of the parameters ν, k, κ, ϵ and C. For Case 3, the values for these parameters are $\nu = 5$, $C = 3$, $k = 1.5$, $\kappa = 3$ and $\epsilon = 0.3$. The corresponding plots for Case 3 are shown in this figure.
- Figure 5: The following values have been chosen for Case 4: $\nu = 1$, $C = 1$, $k = 2$, $\kappa = 1$, $\epsilon = 0.7$.

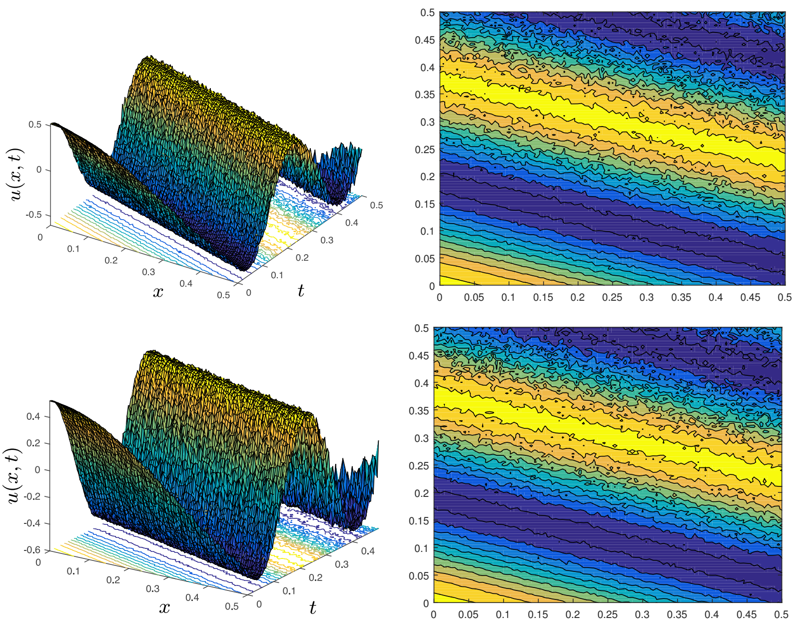

Figure 4. The surface and contour plots of $u(x,t)$ for Case 3.

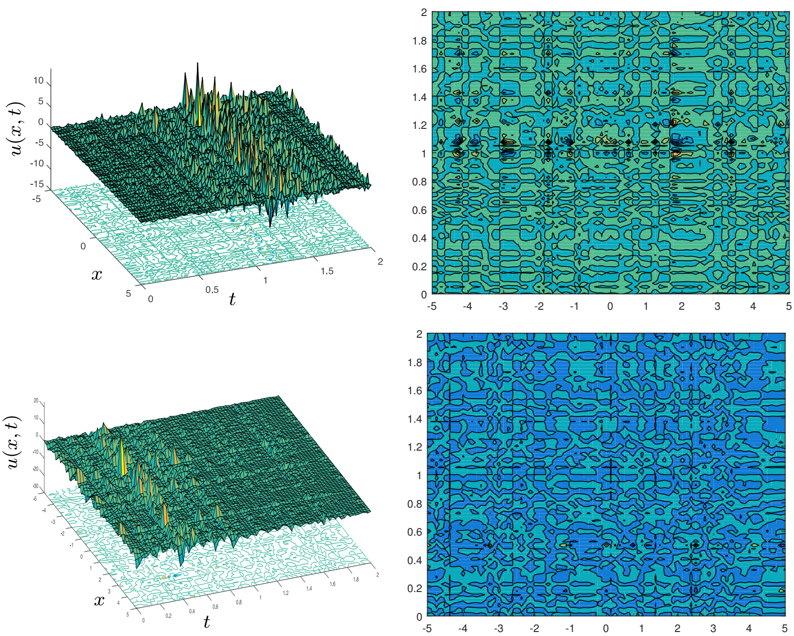

Figure 5. The surface and contour plots of $u(x,t)$ for Case 4.

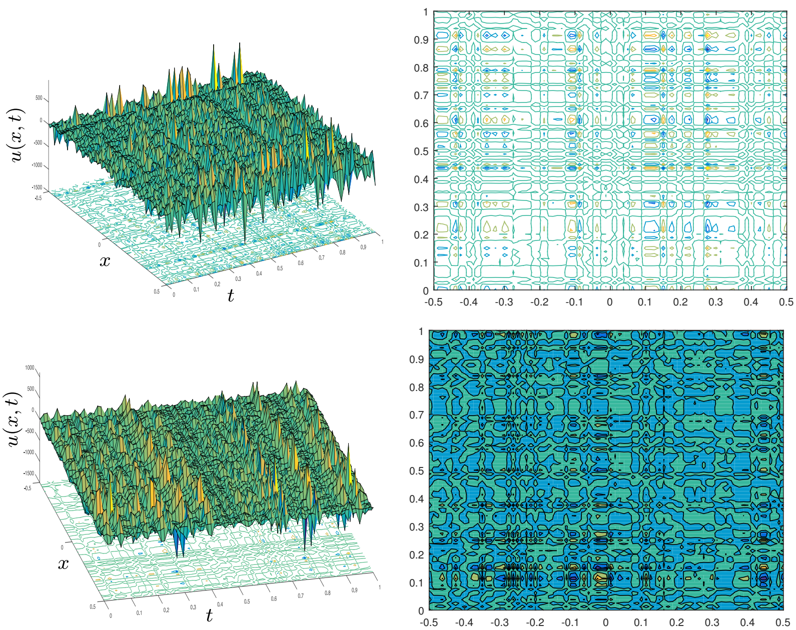

Figure 6. The surface and contour plots of $u(x,t)$ for Case 5.

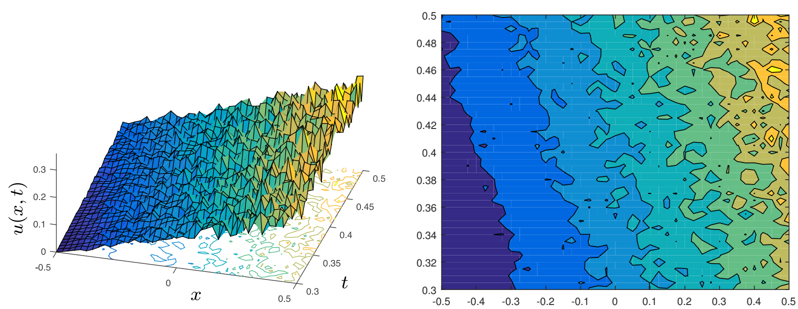

Figure 7. The surface and contour plots of $u(x,t)$ for Case 6.

- Figure 6: For Case 5, we chose $\nu = 4$, $C = 10$, $k = 1$, $\kappa = 4$, $\epsilon = 0.9$, and the graphs are shown in this figure.
- Figure 7: We chose $\nu = 5$, $C = .5$, $k = 4$, $\kappa = 6$ and $\epsilon = .5$. The corresponding plots for Case 6 are shown in this figure.

For the better understanding of the reader, Table 1 has been constructed for the obtained solutions of Case 1. Since, we have obtained the exact solutions and in general no comparisons have been made, such tables are obvious for each case of the obtained solutions.

Table 1

x	t	$u(x,t)$
-2	-0.1	$0.5\,\mathrm{e}^{-0.1245000000+1.037500000\sqrt{12-0.256\,\dot W}}$
-1.5	-0.0375	$0.5\,\mathrm{e}^{-0.09168750000-0.7640625000\sqrt{12-0.256\,\dot W}}$
-1	0.0250	$0.5\,\mathrm{e}^{-0.05887500000-0.4906250000\sqrt{12-0.256\,\dot W}}$
-0.5	0.0875	$0.5\,\mathrm{e}^{-0.02606250000-0.2171875000\sqrt{12-0.256\,\dot W}}$
0	0.15	$0.5\,\mathrm{e}^{0.006750000000+0.05625000000\sqrt{12-0.256\,\dot W}}$
0.5	0.2125	$0.5\,\mathrm{e}^{0.03956250000+0.3296875000\sqrt{12-0.256\,\dot W}}$
1	0.2750	$0.5\,\mathrm{e}^{0.07237500000+0.6031250000\sqrt{12-0.256\,\dot W}}$
1.5	0.3375	$0.5\,\mathrm{e}^{0.1051875000+0.8765625000\sqrt{12-0.256\,\dot W}}$
2	0.40	$0.5\,\mathrm{e}^{0.1380000000+1.150000000\sqrt{12-0.256\,\dot W}}$

Table 2

0.0115	0.0298	0.0724	0.1748	0.4368	1.0761	2.6181	6.4618	15.9255
0.0128	0.0313	0.0785	0.1991	0.4754	1.1766	2.9067	7.4165	16.6205
0.0150	0.0355	0.0855	0.2129	0.5174	1.2620	3.1537	7.7692	18.2876
0.0160	0.0371	0.0929	0.2300	0.5618	1.3590	3.3867	8.6067	19.6727
0.0162	0.0406	0.1040	0.2480	0.6122	1.5086	3.6856	9.0977	21.3715
0.0172	0.0445	0.1119	0.2696	0.6615	1.6212	4.0673	9.6251	25.4104
0.0197	0.0478	0.1207	0.2962	0.7247	1.7843	4.3253	10.1363	25.4948
0.0220	0.0532	0.1285	0.3236	0.7855	1.9253	4.5859	10.9104	28.4565
0.0245	0.0571	0.1397	0.3472	0.8614	2.0600	5.1683	12.6345	31.8407

Since $\dot W$ is a random function, hence from the above chosen values for x and t the values of the function $u(x,t)$ are given in Table 2.

Remark 2. It is worth noting that the simulation of our results are similar to the results published in [33].

6 Conclusion

The mathematical analysis of the partial differential equation (equipped with quadratic singularity and white noise) has been done by using Schauder's fixed point theorem. Moreover, the singularity control with respect to the singularity coefficient ϵ has been verified. The exact solutions to the said problem have been obtained, and the corresponding surface and contour plots for various cases have been drawn.

Acknowledgment. We would like to thank the anonymous reviewers for their critical input to improve this article.

References

1. M.J. Ablowitz, P.A. Clarkson, *Solitons, Nonlinear Evolution Equations and Inverse Scattering*, Cambridge Univ. Press, Cambridge, 1991, `https://doi.org/10.1017/CBO9780511623998`.

2. M.J. Ablowitz, D.J. Kaup, A.C. Newell, H. Segur, Nonlinear-evolution equations of physical significance, *Phys. Rev. Lett.*, **31**(2):125, 1973, https://doi.org/10.1103/PhysRevLett.31.125.
3. P. Debnath, N. Konwar, S. Radenovic, *Metric Fixed Point Theory: Applications in Science, Engineering and Behavioural Sciences*, Springer, Singapore, 2021, https://doi.org/10.1007/978-981-16-4896-0.
4. Z.S. Feng, The first-integral method to study the Burgers–Korteweg–de Vries equation, *J. Phys. A, Math. Gen.*, **35**:343–349, 2002, https://doi.org/10.1088/0305-4470/35/2/312.
5. H. Hassan, M.M. Rashidi, An analytic solution of micropolar flow in a porous channel with mass injection using homotopy analysis method, *Int. J. Numer. Methods Heat Fluid Flow*, **24**(2):419–437, 2014, https://doi.org/10.1108/HFF-08-2011-0158/full/html.
6. J. He, A new approach to nonlinear partial differential equations, *Commun. Nonlinear Sci. Numer. Simul.*, **2**:230–235, 1997, https://doi.org/10.1016/S1007-5704(97)90007-1.
7. J. He, An approximate solution technique depending on an artificial parameter: A special example, *Commun. Nonlinear Sci. Numer. Simul.*, **3**:92–97, 1998, https://doi.org/10.1016/S1007-5704(98)90070-3.
8. R. Hirota, Exact solution of the Korteweg–de Vries equation for multiple collisions of solitons, *Phys. Rev. Lett.*, **27**:1192–1194, 1971, https://doi.org/10.1103/PhysRevLett.27.1192.
9. M.S. Iqbal, *Solutions of Boundary Value Problems for Nonlinear Partial Differential Equations by Fixed Point Methods*, PhD thesis, Technische Universität Graz, 2011.
10. K. Khan, M.A. Akbar, Solitary wave solutions of some coupled nonlinear evolution equations, *J. Sci. Res.*, **6**:273–284, 2014, https://doi.org/10.3329/jsr.v6i2.16671.
11. K. Khan, M.A. Akbar, Study of analytical method to seek for exact solutions of variant Boussinesq equations, *SpringerPlus*, **3**:324, 2014, https://doi.org/10.1186/2193-1801-3-324.
12. K. Khan, M.A. Akbar, Traveling wave solutions of the $(2+1)$-dimensional Zoomeron equation and the Burgers equations via the MSE method and the Exp-function method, *Ain Shams Eng. J.*, **5**:247–256, 2014, https://doi.org/10.1016/j.asej.2013.07.007.
13. K. Khan, M.A. Akbar, S.M.R. Islam, Exact solutions for $(1 + 1)$-dimensional nonlinear dispersive modified Benjamin–Bona–Mahony equation and coupled Klein–Gordon equations, *SpringerPlus*, **3**:724–731, 2014, https://doi.org/10.1186/2193-1801-3-724.
14. T. Lei, G. Chen, Dominant dynamics for a class of singularly perturbed stochastic partial differential equations with quadratic nonlinearities and random Neumann boundary conditions, *Chaos*, **31**(7):073109, 2021, https://doi.org/10.1063/5.0042117.
15. B.C. Lin, Extended homogeneous balance method and Lax pairs, Bäcklund transformation, *Commun. Theor. Phys.*, **37**:645–648, 2002, https://doi.org/10.1088/0253-6102/37/6/645.
16. B. Lu, The first integral method for some time fractional differential equations, *J. Math. Anal. Appl.*, **395**:684–693, 2012, https://doi.org/10.1016/j.jmaa.2012.05.066.

17. C. Rogers, W.K. Schief, *Bäcklund and Darboux Transformation Geometry and Modern Applications in Solitons Theory*, Cambridge Univ. Press, Cambridge, 2002, https://doi.org/10.1017/CBO9780511606359.
18. S. Sarwar, M.M. Rashidi, Approximate solution of two-term fractional-order diffusion, wave-diffusion, and telegraph models arising in mathematical physics using optimal homotopy asymptotic method, *Waves Random Complex Media*, **26**(3):365–382, 2016, https://doi.org/10.1080/17455030.2016.1158436.
19. H. Shahmohamadi, M.M. Rashidi, VIM solution of squeezing MHD nanofluid flow in a rotating channel with lower stretching porous surface, *Adv. Powder Technol.*, **27**(1):171–178, 2016, https://doi.org/10.1016/j.apt.2015.11.014.
20. X. Si-Liu, L. Jian-Chu, Y. Lin, Exact soliton solutions to a generalized nonlinear Schrödinger equation, *Commun. Theor. Phys.*, **53**:159–165, 2010, https://doi.org/10.1088/0253-6102/53/1/33.
21. N. Taghizadeh, M. Mirzazadeh, T. Filiz, The first-integral method applied to the Eckhaus equation, *Appl. Math. Lett.*, **25**:798–802, 2012, https://doi.org/10.1016/j.aml.2011.10.021.
22. M. Wang, Solitary wave solutions for variant Boussinesq equations, *Phys. Lett. A*, **199**:169–172, 1995, https://doi.org/10.1016/0375-9601(95)00092-H.
23. M. Wang, X. Li, Applications of F-expansion to periodic wave solutions for a new Hamiltonian amplitude equation, *Chaos Solitons Fractals*, **24**:1257–1268, 2005, https://doi.org/10.1016/j.chaos.2004.09.044.
24. M. Wang, X. Li, J. Zhang, The $(\frac{G'}{G})$-expansion method and travelling wave solutions of nonlinear evolution equations in mathematical physics, *Phys. Lett. A*, **372**:417–423, 2008, https://doi.org/10.1016/j.physleta.2007.07.051.
25. M. Wang, Y. Zhou, Z. Li, Application of a homogeneous balance method to exact solutions of nonlinear equations in mathematical physics, *Phys. Lett. A*, **216**:67–75, 1996, https://doi.org/10.1016/0375-9601(96)00283-6.
26. Z. Wang, X. Huan, K. Garikipati, Variational system identification of the partial differential equations governing the physics of pattern-formation: Inference under varying fidelity and noise, *Comput. Methods Appl. Mech. Eng.*, **356**(1):44–74, 2019, https://doi.org/10.1016/j.cma.2019.07.007.
27. Z. Wang, X. Huan, K. Garikipati, Variational system identification of the partial differential equations governing microstructure evolution in materials: Inference over sparse and spatially unrelated data, *Comput. Methods Appl. Mech. Eng.*, **377**:113706, 2021, https://doi.org/10.1016/j.cma.2021.113706.
28. A.M. Wazwaz, The tanh method: Exact solutions of the sine-Gordon and the sinh-Gordon equations, *Appl. Math. Comput.*, **167**:1196–1210, 2005, https://doi.org/10.1016/j.amc.2004.08.005.
29. G. Wei, A new algorithm for solving some mechanical problems, *Comput. Methods Appl. Mech. Eng.*, **190**(15-17):2017–2030, 2001, https://doi.org/10.1016/S0045-7825(00)00219-X.
30. Z. Yan, Abundant families of Jacobi elliptic function solutions of the-dimensional integrable Davey–Stewartson-type equation via a new method, *Chaos Solitons Fractals*, **18**:299–309, 2003, https://doi.org/10.1016/S0960-0779(02)00653-7.

31. X.F. Yang, Z.C. Deng, Y. Wei, A Riccatti–Bernoulli sub-ODE method for nonlinear partial differential equations and its application, *Adv. Contin. Discrete Models*, **2015**(1):1–17, 2015, https://doi.org/10.1186/s13662-015-0452-4.
32. X.F. Yang, Y. Wei, Bilinear equation of the nonlinear partial differential equation and its application, *J. Funct. Spaces*, **2020**, 2020, https://doi.org/10.1155/2020/4912159.
33. M.W. Yasin, M.S. Iqbal, N. Ahmed, A. Akgül, A. Raza, M. Rafiq, M.B. Riaz, Numerical scheme and stability analysis of stochastic Fitzhugh–Nagumo model, *Results Phys.*, **32**: 105023, 2022, https://doi.org/10.1016/j.rinp.2021.105023.
34. E. Yusufoglu, The variational iteration method for studying the Klein–Gordon equation, *Appl. Math. Lett.*, **21**:669–674, 2008, https://doi.org/10.1016/j.aml.2007.07.023.
35. H. Zhang, New application of the $(\frac{G'}{G})$-expansion method, *Commun. Nonlinear Sci. Numer. Simul.*, **14**:3220–3225, 2009, https://doi.org/10.1016/j.cnsns.2009.01.006.